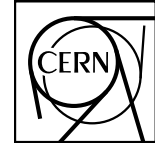


# Laser excitation of the $n=3$ level of positronium

S. Aghion<sup>1,2</sup>, C. Amsler<sup>3</sup>, A. Ariga<sup>3</sup>, T. Ariga<sup>3</sup>, G. Bonomi<sup>4,5</sup>, P. Brüning<sup>6</sup>, T. Dörmann<sup>7</sup>, D. C. Dörmann<sup>8,9</sup>, T. Cabaret<sup>10</sup>, M. Caccia<sup>2,11</sup>, R. Caravita<sup>12,13</sup>, F. Castelli<sup>2,14</sup>, G. Cerchi Comparat<sup>10</sup>, G. Consolati<sup>1,2</sup>, A. Demetrio<sup>6</sup>, L. Di Noto<sup>12,13</sup>, M. Doser<sup>7</sup>, A. Ferragut<sup>1,2</sup>, J. Fesel<sup>7</sup>, A. Fontana<sup>5</sup>, O. K. Forslund<sup>7</sup>, S. Gerber<sup>7</sup>, M. Gianfranceschi<sup>15</sup>, F. Guatieri<sup>8,9</sup>, S. Haider<sup>7</sup>, H. Holmestad<sup>19</sup>, T. Huse<sup>19</sup>, I. L. Jernelv Kellerbauer<sup>15</sup>, M. Kimura<sup>3</sup>, T. Koetting<sup>7</sup>, D. Krasnicky<sup>12,13</sup>, V. Lagomarsino<sup>15</sup>, Lehner<sup>20</sup>, J. Liberadzka<sup>7</sup>, C. Malbrunot<sup>7,20</sup>, S. Mariazzi<sup>20,\*</sup>, L. Marx<sup>7</sup>, M. Nebbia<sup>22</sup>, P. Nedelec<sup>23</sup>, M. Oberthaler<sup>6</sup>, N. Pacifico<sup>17</sup>, D. Pagano<sup>4,5</sup>, L. Prell<sup>2</sup>, M. Prevedelli<sup>24</sup>, L. Ravelli<sup>8,9</sup>, L. Resch<sup>7</sup>, B. Rienacker<sup>7</sup>, O.M. Røhne<sup>19</sup>, S. Rosenberger<sup>7</sup>, A. Rotondi<sup>5,25</sup>, M. Sacerdoti<sup>2,14</sup>, H. Sandaker<sup>19</sup>, R. Santoro<sup>2,11</sup>, P. Scamporrino<sup>3,26</sup>, F. Sorrentino<sup>12,13</sup>, M. Spacek<sup>16</sup>, J. Storey<sup>3</sup>, I. M. Strojek<sup>16</sup>, G. Testera<sup>13</sup>, I. Tietje<sup>7</sup>, S. Vamori<sup>20</sup>, E. Widmann<sup>20</sup>, P. Yzombard<sup>10</sup>, S. Zavatarelli<sup>13</sup>, and J. Zmeskal<sup>20</sup>



CERN-PH-EP-2015-265  
23 September 2015

1]Politecnico of Milano, Piazza Leonardo da Vinci 32, 20133 Milano, Italy

2]INFN Milano, via Celoria 16, 20133 Milano, Italy

3]Laboratory for High Energy Physics, Albert Einstein Center for Fundamental Physics, University of Bern, 3012 Bern, Switzerland

4]Department of Mechanical and Industrial Engineering, University of Brescia, via Branze 38, 25123 Brescia, Italy

5]INFN Pavia, via Bassi 6, 27100 Pavia, Italy

6]Kirchhoff-Institute for Physics, Heidelberg University, Im Neuenheimer Feld 227, 69120 Heidelberg, Germany

7]Physics Department, CERN, 1211 Geneva 23, Switzerland

8]Department of Physics, University of Trento, via Sommarive 14, 38123 Povo, Trento, Italy

9]TIFPA/INFN Trento, via Sommarive 14, 38123 Povo, Trento, Italy

10]Laboratoire Aimé Cotton, Université Paris-Sud, ENS Cachan, CNRS, Université Paris-Saclay, 91405 Orsay Cedex, France

11]Department of Science, University of Insubria, Via Valleggio 11, 22100 Como, Italy

12]Department of Physics, University of Genova, via Dodecaneso 33, 16146 Genova, Italy

13]INFN Genova, via Dodecaneso 33, 16146 Genova, Italy

14]Department of Physics, University of Milano, via Celoria 16, 20133 Milano, Italy

15]Max Planck Institute for Nuclear Physics, Saupfercheckweg 1, 69117 Heidelberg, Germany

16]Czech Technical University, Prague, Bøheřová 7, 11519 Prague 1, Czech Republic

17]Institute of Physics and Technology, University of Bergen, Alleegaten 55, 5007 Bergen, Norway

18]Institute for Nuclear Research of the Russian Academy of Science, Moscow 117312, Russia

19]Department of Physics, University of Oslo, Semælands vei 24, 0371 Oslo, Norway

20]Stefan Meyer Institute for Subatomic Physics, Austrian Academy of Sciences, Boltzmannngasse 3, 1090 Vienna, Austria

21]Joint Institute for Nuclear Research, 141980 Dubna, Russia

22]INFN Padova, via Marzolo 8, 35131 Padova, Italy

23]Institute of Nuclear Physics, CNRS/IN2p3, University of Lyon 1, 69622 Villeurbanne, France

24]University of Bologna, Viale Berti Pichat 6/2, 40126 Bologna, Italy

25]Department of Physics, University of Pavia, via Bassi 6, 27100 Pavia, Italy

26]Department of Physics, University of Napoli Federico II, Complesso Universitario di Monte S. Angelo, 80126, Napoli, Italy

(AEgIS Collaboration)

(Dated: September 17, 2015)

We demonstrate laser excitation of the  $n=3$  state of positronium (Ps) in vacuum. A specially designed high-efficiency pulsed slow positron beam and single shot positronium annihilation lifetime spectroscopy were used to produce and detect Ps. Pulsed laser excitation of  $n=3$  level at 205 nm was monitored via Ps photoionization induced by a second intense laser pulse at 1064 nm. About 15% of the overall positronium emitted in vacuum was excited to  $n=3$  and photoionized. Saturation of both the  $n=3$  excitation and the following photoionization was observed and is explained by a simple rate equation model. Scanning the laser frequency allowed us to extract the positronium transverse temperature related to the width of the Doppler-broadened line. Moreover, preliminary observation of excitation to Rydberg states ( $n = 15 \dots 17$ ) using  $n=3$  as intermediate level was observed, giving an independent confirmation of efficient excitation to the  $3^3P$  state.

**PACS numbers:** 32.80.Rm, 36.10.Dr, 78.70.Bj

\* Corresponding author: Sebastiano.Mariazzi@cern.ch

Positronium is a purely leptonic hydrogen-like bound state composed of an electron ( $e^-$ ) and its antiparticle, the positron ( $e^+$ ). Ps has two ground states: the triplet  $1^3S$  state (ortho-positronium, o-Ps, that annihilates predominantly into three photons with a lifetime of 142 ns in vacuum) and the singlet  $1^1S$  state (para-positronium, p-Ps, annihilating predominantly into two photons with a lifetime of 125 ps). Since its discovery in 1951, Ps has become a testing ground of bound-state QED [1]. Up to now, only the excited levels  $n=2$  and the Rydberg  $n=10-31$  have been experimentally observed [2–6]. Efficient laser excitation of o-Ps is a very useful spectroscopic tool [7], to study or modify the Ps formation [8, 9], for antihydrogen formation [10–13] or for preparation of selected states for further manipulation [6, 14, 15].

Here we present the first observation via laser excitation and photoionization of the Ps  $n=3$  level that has been achieved with an overall efficiency of  $\sim 15\%$ . Excitation to this level is of interest for spectroscopy, but also for antihydrogen formation as proposed by the AEGIS [16, 17] and by the GBAR experiments [18, 19]. An enhanced antihydrogen formation rate, via collisions with cold antiprotons, is expected to occur when Ps is excited to  $n=3$  [20–22]. Moreover, excitation of the Ps  $n=3$  level is also of high interest to produce efficiently the metastable  $2^3S$  state after spontaneous decay, as was achieved with a hydrogen beam [23]. This could open the way to new high precision measurements of the  $1^3S-2^3S$  transition [24] and to experiments using Ps atomic beams with long lifetime for interferometric measurements [23].

Positrons, emitted by a 11 mCi  $^{22}\text{Na}$  source, were prepared by a Surko-style trap [25] and accumulator. After rotating-wall compression [26], 20 ns bunches containing  $3 \times 10^7$  positrons each were produced by fast-switched electric potentials and transported to a magnetic-field-free region. There they were recompressed with a 24-electrode buncher into a pulse of about 7 ns and accelerated into a nanochanneled silicon target at 3.3 keV kinetic energy. Here, bunches of  $e^+$  are efficiently converted into o-Ps and emitted in vacuum [27, 28]. Using a calibrated CsI detector and a MicroChannel Plate (MCP) plus phosphor screen in place of the silicon target, it was estimated that 30 – 40% of  $e^+$  dumped from the accumulator hit the sample in a spot of less than 4 mm FWTM. Two symmetric coils allow the tuning of a longitudinal magnetic field in the sample region to induce o-Ps quenching. Experiments presented here have been performed in a 600 V/cm electric and 0.025 T magnetic field environment. The magnetic field is set perpendicular to the target. For a more detailed description of this system and its performances see Refs. [29] and [30].

Ps formed in the target and emitted into vacuum was detected by using the single shot  $e^+$  annihilation lifetime spectroscopy (SSPALS) technique [31]. A 20x25x25 mm lead tungstate ( $\text{PbWO}_4$ ) scintillator coupled to a Hamamatsu R11265-100 PhotoMultiplier Tube (PMT) was placed at a distance of 4 cm above the sample and recorded  $\gamma$ -rays emitted in positron-electron anni-

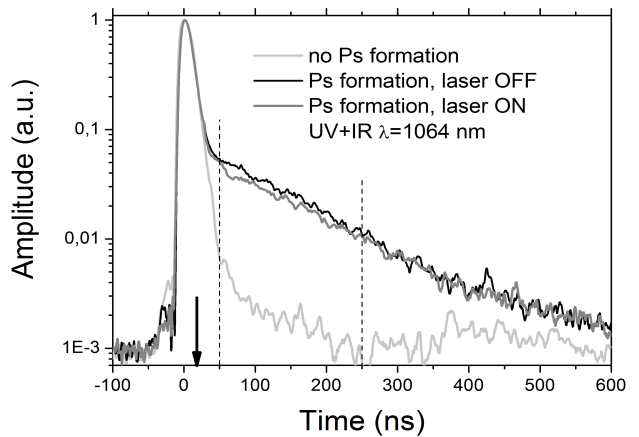


FIG. 1. SSPALS spectra of: background (light gray line), Ps into vacuum with laser OFF (black line) and laser UV+IR (1064 nm) ON (dark gray line). Each spectrum is composed by the average of 15 single shots. The arrow marks the time of laser shot on the Ps cloud (16 ns after prompt peak). Area between 50 ns and 250 ns from the prompt peak (vertical dashed lines) has been considered for evaluation of  $S$  for  $n=3$  (see text).

hilations. To enhance resolution at the longest decay times, the signal from the PMT was split and sent to two channels of a 500 MHz oscilloscope with high (100 mV/division) and low (1 V/division) gain. Joined data from the two channels give the SSPALS spectra shown in Fig. 1 when  $e^+$  are bunched on the surface of the MCP (no Ps formation; background) and on the target (Ps formation). Following our initial proposal to use the  $n=3$  state as an intermediate state towards Rydberg excitation for the AEGIS experiment [16], we have developed a pulsed laser system capable of efficiently saturating the  $1^3S - 3^3P$  transition. This broadband laser system [14] produces pulses covering most of the Zeeman mixing and Doppler broadening of the transition in the cryogenic environment of AEGIS. Covering the rather large Doppler linewidth at room temperature by the laser pulse spectrum is challenging. Nevertheless, saturation of the  $1S-2P$  transition has been reached in Ps under similar conditions thanks to power broadening [32]. In our case the effect is expected to be less pronounced due to the smaller natural linewidth of the transition.

The laser setup is described in detail in Ref. [33]. In normal working conditions, the laser system was able to deliver 54  $\mu\text{J}$  pulses of ultra-violet (UV) light to the experimental room-temperature chamber, in a wavelength range from 204 nm to 206 nm. The wavelength was tuned by adjusting the temperature of an Optical Parametric Generator (OPG) crystal. The pulse has vertical polarization, a nearly-gaussian temporal profile with a FWHM of  $t \sim 1.5$  ns, a gaussian spectral profile with sigma  $\sigma_{\text{laser}} \approx 2\pi \times 48$  GHz and a slightly elliptical gaussian spatial shape, with  $\text{FWHM}_{\text{vertical}} = 6$  mm and  $\text{FWHM}_{\text{horizontal}} = 4$  mm. A second, intense infrared (IR) laser pulse at 1064 nm was simultaneously delivered to

the experimental chamber. This pulse has an energy of 50 mJ and a temporal FWHM of 10 ns, and it is horizontally polarized. It was superimposed to the 205 nm pulse both in time, with a precision of 1 ns with an optical delay line, and in space by increasing its size so as to completely cover the excitation pulse area (top-hat profile of 8 mm diameter). Both beams were aligned on the target region by monitoring their position with a CCD camera on a 1-inch Macor<sup>®</sup> screen placed inside the vacuum region, a few cm away from the target. A mutual synchronization of positrons and laser pulses with a time resolution of 2 ns and a jitter of less than 600 ps was obtained by a custom Field Programmable Gate Array (FPGA) based synchronization device. The time delay between the prompt positron annihilation peak and the laser pulses was set to 16 ns (vertical arrow in Fig. 1).

The fraction of excited o-Ps was measured by analyzing the decrease in the annihilation rate in the SSPALS spectra induced by populating the  $3^3P$  state. Two methods can be used for this purpose: quenching in a magnetic field (i) or photoionization with the IR laser pulse (ii). In absence of magnetic field  $3P$  states decay radiatively to the ground state in 10.5 ns. In presence of a magnetic field (i) the  $3^3P$  state is Zeeman-mixed with the  $3^1P$  state and can decay toward the  $1^1S$  state, subsequently annihilating with a lifetime of 125 ps into two  $\gamma$ -rays. Otherwise (ii), photoionization of the  $3^3P$  state dissociates the Ps and the free positrons are quickly accelerated toward the last negative electrode of our set up, where they annihilate. Whichever technique is chosen, both processes result in a decrease of the o-Ps population decaying into three  $\gamma$ s. The fraction of excited o-Ps can be evaluated by analyzing the decrease in the area below the SSPALS spectra when quenching or photoionization are applied. The fraction  $S$  of quenched or ionized o-Ps atoms was evaluated from the areas  $f_{\text{off}}$  and  $f_{\text{on}}$  of the SSPALS spectra, with UV laser off and on, between 50 ns and 250 ns from the prompt peak:  $S=(f_{\text{off}}-f_{\text{on}})/f_{\text{off}}$ .

We used a simulation code which performs the numerical diagonalization of the full interaction Hamiltonian in electric and magnetic fields [32] to predict the value of the external field required to get the maximum magnetic quenching efficiency. We then set a 0.025 T magnetic field in the sample region and measured the quenching efficiency following the  $n=3$  excitation. We observed a maximum reduction through quenching of  $S=3.6 \pm 1.2$  %. When applying the IR pulse for photoionization, a decrease of o-Ps annihilations becomes plainly visible in the SSPALS spectrum of Fig. 1, corresponding to a value of 15% for the  $S$  parameter. The ratio of the two efficiencies is in good agreement with the one given by the simulation code.

We have scanned the UV wavelength using an Avantes AvaSpec-3648-USB2 wavemeter (accuracy =  $\pm 0.02$  nm). At each wavelength the mean  $S$  value and its standard deviation were calculated for a sample of 15 shots (Fig. 2). A fit (see below) gives the  $3P$  excitation line central value of  $205.05 \pm 0.02$  nm. The calculated theoretical

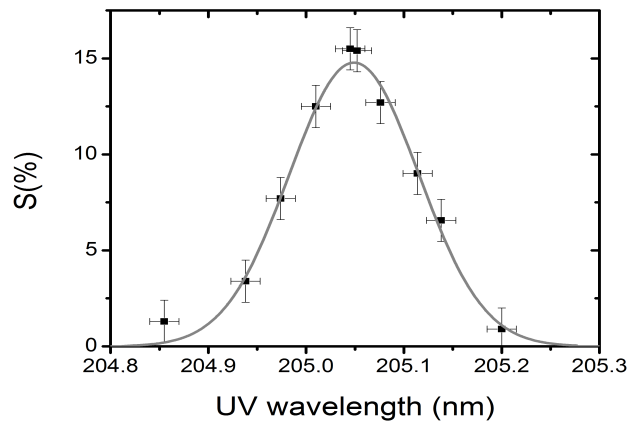


FIG. 2. Linewidth of the  $1^3S - 3^3P$  Ps excitation obtained by scanning the UV laser wavelength for constant IR wave length. Each point has been calculated by averaging 15 SSPALS spectra. Statistical errors (on y axis) and accuracy (on x axis) are reported (see text). The continuous line is a fit obtained with Eq.(3).

expected value is 205.0474 nm [34].

The saturation energies of both  $1S-3P$  and  $3P$ -ionization transitions have been studied (see Fig. 3). The  $1S-3P$  transition results only slightly saturated, while the  $3P$ -continuum is strongly saturated. This means that almost all of  $n=3$  atoms are photoionized as soon as they get excited. Thus, the  $S$  value can directly be seen as the excitation efficiency. From our data we conclude that  $\sim 15\%$  of the overall positronium emitted in vacuum has been excited into  $n = 3$  state, and subsequently photoionized.

To analyze these results, as described below, we used a simple 3 level rate equation model which neglects spontaneous emission and assumes that the laser pulses are constant over the pulse time  $t$ . At strong IR intensity the  $n = 3$  states are almost instantaneously photoionized. This leads to a probability for Ps( $n = 3$ ) photoionization:

$$p(t, \mathbf{r}, \mathbf{v}, \delta) = 1 - e^{-\gamma t} \quad (1)$$

where  $\gamma$  is the UV absorption rate. Our laser spectrum has a linewidth ( $\sigma_{\text{laser}}$ ) much larger than the ionization rate and of both the natural linewidth and the hyperfine splitting structure (3 GHz), hence:

$$\gamma(\mathbf{v}, \mathbf{r}, \delta) \approx \frac{\pi \Omega(\mathbf{r})^2}{2} \frac{1}{\sqrt{2\pi\sigma_{\text{laser}}^2}} e^{-(\delta - \mathbf{k} \cdot \mathbf{v})^2 / 2\sigma_{\text{laser}}^2} \quad (2)$$

where  $\delta$  is the laser frequency detuning with respect to resonance with Ps at rest ( $\mathbf{v}$  being the Ps velocity),  $\mathbf{k}$  is the UV laser wave-number and  $\Omega(\mathbf{r})$  is the Rabi frequency that depends on the position  $\mathbf{r}$  of the Ps atoms inside the laser beam. Spatial averaging with the (gaussian) Ps density profile can then be performed. For our moderate saturation, we found more meaningful to extrapolate the spatial averaging result - valid at low saturation (where  $p \approx \gamma t$ ) - by defining a geometrical overlapping efficiency

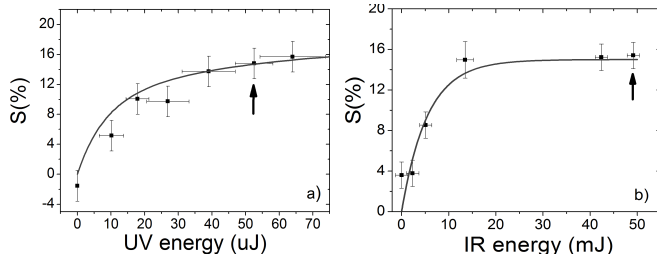


FIG. 3. S parameter (as defined in the text) in function of: UV energy (IR energy = 50 mJ) a) and IR energy (UV energy = 54  $\mu$ J) b). Arrows mark the laser energies used for the measurements of Fig.1 and 2. The continuous lines are fits from the 3 levels rate equation model (see text).

coefficient  $\eta$  and thus  $\Omega$  is replaced by its peak value. The probability of photo-ionization, assuming a Ps cloud at temperature  $T$ , is then given by:

$$P(t, \delta) = \eta \int_{-\infty}^{+\infty} p(t, v, \delta) \sqrt{\frac{1}{2\pi\sigma_v^2}} e^{-\frac{v^2}{2\sigma_v^2}} dv \quad (3)$$

where  $\sigma_v = \sqrt{k_B T/m}$  is the standard deviation of the velocity along the laser propagation axis. This formula has been used to fit the data in Fig. 2 and Fig. 3 a). We find  $\Omega^2 \sim 8 \times 10^{10} s^{-1} \times \frac{\text{Energy}}{\mu\text{J}} \times \frac{1}{t_{UV\text{pulse}}}$  corresponding to a dipole strength  $d=1.70$  Debye, in good agreement with the theoretical value of 1.65 D predicted in Ref. [16].

The Fig.2 lineshape is almost entirely dominated by the thermal distribution of the Ps, so we obtain an o-Ps velocity in the transverse direction of  $\sigma_v \approx 10^5$  m/s, or a temperature  $T \approx 1300$  K, in agreement with previous observations of fast thermal emission from similar targets at low positron implantation energy [28, 35]. We also find a large geometrical overlap of  $\eta \sim 80\%$ , in reasonable agreement with the 60% found by a simulation of Ps excitation during expansion in vacuum [36].

From our model we deduce that the laser spatial and temporal overlap with the Ps cloud is very good and that the 15% Ps excitation-photoionization efficiency is mainly due to the near 10% ratio of laser spectral linewidth  $\sigma_{\text{laser}} = 2\pi \times 48$  GHz to the Doppler width  $k\sigma_v = 2\pi \times 470$  GHz; the power broadening has to be taken into account to explain the larger efficiency value of 15%.

Finally we used the rate equation model to fit the data in Fig 3 b) and found a maximum ionization rate of  $2.9 \times 10^9 s^{-1}$ , corresponding to a photoionization cross section by the 1064 nm photons of  $\sim 1.8 \times 10^{-16} \text{ cm}^2$ .

An independent test to demonstrate excitation of  $3^3\text{P}$  level was performed by using an IR laser beam, suitable for exciting Ps Rydberg levels. A first demonstration of Rydberg excitation using  $3^3\text{P}$  as intermediate level is carried out by simply varying the wavelength of the IR pulse. Rydberg excitation increases the o-Ps lifetime, allowing a large number of o-Ps to reach the walls of the

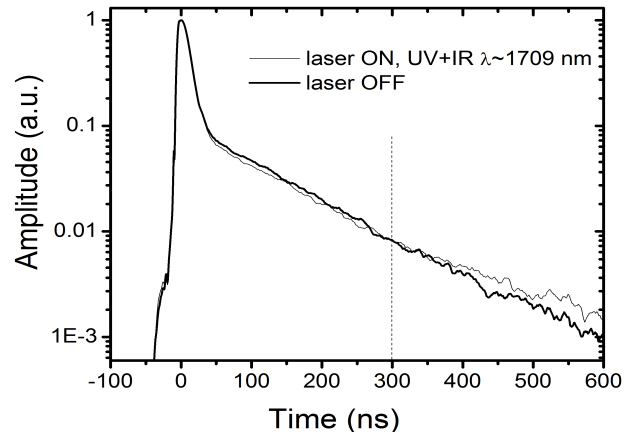


FIG. 4. SSPALS spectra of Ps into vacuum with laser OFF (black line) and laser UV+IR (1709 nm) ON (dark gray line). Shown spectra are composed by averaging 40 single shots. Area between 300 ns (vertical dashed line) and 600 ns from the prompt peak has been considered for evaluation of S for Rydberg levels (see text).

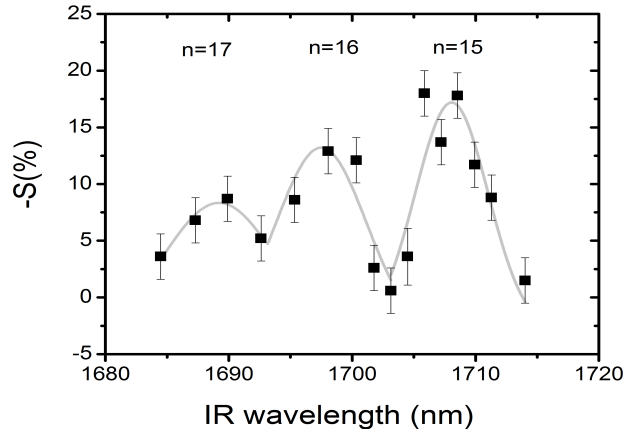


FIG. 5. Scan of the S parameter versus the IR wavelength in the range  $n=15\dots17$ . An eye-guide is shown in gray. Data are taken by averaging 15 SSPALS spectra.

vacuum chamber. As a consequence, the SSPALS spectra show a decrease of annihilations immediately after the laser shot and an increase at long times after the  $1^1\text{S}$  annihilation peak (Fig.4). The Rydberg excitation signal can be extracted from SSPALS spectra by calculating the S parameter in the time window between 300 ns and 600 ns after the prompt positron annihilation peak. A scan of the IR laser wavelength was carried out for exciting Ps from  $n=3$  to levels between  $n=15$  and  $n=17$ . The UV laser wavelength was kept constant on resonance of  $n=3$ .

The behavior of the S as a function of the IR wavelength is shown in Fig.5. Despite the broadening of the combined 600 V/cm electric and 0.025 T magnetic fields, the  $n=15$  level was clearly distinguishable; for higher states, different n-manifolds start to overlap in a continuum of energy levels. Results obtained in this scan are in good agreement with the spectroscopic survey carried

out in Ref.[4] using  $2^3\text{P}$  as intermediate level.

To summarize, in the present work we have demonstrated the first laser excitation of Ps to the  $n=3$  state. The excitation-photoionization efficiency of  $\sim 15\%$  is mainly limited by the ratio of the laser linewidth to the Doppler broadening of the Ps line. Reduction of the o-Ps emission velocity from the target is thus an obvious way to enhance the excitation efficiency. A preliminary Rydberg excitation using  $3^3\text{P}$  as intermediate level has also been shown, opening the possibility to further studies involving  $n=3$ -Rydberg transitions [37].

## ACKNOWLEDGMENTS

This work was supported by: DFG research grant, excellence initiative of Heidelberg University, ERC under the European Unions Seventh Framework Program (FP7/2007-2013)/ ERC Grant agreement no. (291242) and no. (277762), Austrian Ministry for Science, Research and Economy, Research Council of Norway, Bergen Research Foundation, Istituto Nazionale di Fisica Nucleare (INFN-Italy), John Templeton Foundation, Ministry of Education and Science of the Russian Federation and Russian Academy of Sciences, European social fund within the framework of realizing the project: Support of inter-sectoral mobility and quality enhancement of research teams at Czech Technical University in Prague, CZ.1.07/2.3.00/30.0034.

- 
- [1] S. G. Karshenboim, Phys. Rep. **422**, 1 (2005).
  - [2] S. Chu and A. P. Mills, Phys. Rev. Lett. **48**, 1333 (1982).
  - [3] K. P. Ziock, R. H. Howell, F. Magnotta, R. A. Failor, and K. M. Jones, Phys. Rev. Lett. **64**, 2366 (1990).
  - [4] D. B. Cassidy, T. H. Hisakado, H. W. K. Tom, and A. P. Mills, Phys. Rev. Lett. **108**, 043401 (2012).
  - [5] A. C. L. Jones, T. H. Hisakado, H. J. Goldman, H. W. K. Tom, A. P. Mills, and D. B. Cassidy, Phys. Rev. A **90**, 012503 (2014).
  - [6] T. E. Wall, A. M. Alonso, B. S. Cooper, A. Deller, S. D. Hogan, and D. B. Cassidy, Phys. Rev. Lett. **114**, 173001 (2015).
  - [7] D. B. Cassidy, T. H. Hisakado, H. W. K. Tom, and A. P. Mills, Phys. Rev. Lett. **109**, 073401 (2012).
  - [8] D. B. Cassidy, M. W. J. Bromley, L. C. Cota, T. H. Hisakado, H. W. K. Tom, and A. P. Mills, Phys. Rev. Lett. **106**, 023401 (2011).
  - [9] D. B. Cassidy, T. H. Hisakado, H. W. K. Tom, and A. P. Mills, Phys. Rev. Lett. **106**, 133401 (2011).
  - [10] M. Charlton, J. Eades, D. Horváth, R. Hughes, and C. Zimmermann, Phys. Rep. **241**, 65 (1994).
  - [11] E. A. Hessels, D. M. Homan, and M. J. Cavagnero, Phys. Rev. A **57**, 1668 (1998).
  - [12] Storry, C. H. et al., (ATRAP Collaboration), Phys. Rev. Lett. **93**, 263401 (2004).
  - [13] G. Y. Drobyshev et al., (AEgIS collaboration), Tech. Rep. SPSC-P-334. CERN-SPSC-2007-017 (CERN, Geneva, 2007).
  - [14] M. Becucci, G. Ferrari, I. Boscolo, F. Castelli, S. Cialdi, F. Villa, and M. Giammarchi, J. Mol. Struct. **993**, 495 (2011).
  - [15] D. B. Cassidy and S. D. Hogan, Int. J. Mod. Phys.: Conf. Ser. **30**, 1460259 (2014).
  - [16] F. Castelli, I. Boscolo, S. Cialdi, M. G. Giammarchi, and D. Comparat, Phys. Rev. A **78**, 052512 (2008).
  - [17] M. Doser et al., (AEgIS collaboration), Classical Quantum Gravity **29**, 184009 (2012).
  - [18] P. Perez and Y. Sacquin, Classical Quantum Gravity **29**, 184008 (2012).
  - [19] P. Perez et al., (GBAR collaboration), Hyperfine Interact. (2015).
  - [20] P. Comini and P.-A. Hervieux, New J. Phys. **15**, 095022 (2013).
  - [21] P. Comini, P.-A. Hervieux, and F. Biraben, Hyperfine Interact. (2014).
  - [22] A. Kadyrov, C. Rawlins, A. Stelbovics, I. Bray, and M. Charlton, Phys. Rev. Lett. **114**, 183201 (2015).
  - [23] K. C. Harvey, J. Appl. Phys. **53**, 3383 (1982).
  - [24] D. Cooke, P. Crivelli, J. Alnis, A. Antognini, B. Brown, S. Friedreich, A. Gabard, T. Haensch, K. Kirch, A. Rubbia, and V. Vrankovic, Hyperfine Interact. , 1 (2015).
  - [25] J. R. Danielson, D. H. E. Dubin, R. G. Greaves, and C. M. Surko, Rev. Mod. Phys. **87**, 247 (2015).
  - [26] R. G. Greaves and C. M. Surko, Phys. Rev. Lett. **85**, 1883 (2000).
  - [27] S. Mariazzi, P. Bettotti, S. Larcheri, L. Toniutti, and R. S. Brusa, Phys. Rev. B **81**, 235418 (2010).
  - [28] S. Mariazzi, P. Bettotti, and R. S. Brusa, Phys. Rev. Lett. **104**, 243401 (2010).
  - [29] L. Penasa, L. Di Noto, M. Bettonte, S. Mariazzi, G. Nebbia and R. S. Brusa, J. of Phys.: Conf. Ser. **505**, 012031 (2014).
  - [30] S. Aghion et al., (AEgIS collaboration), submitted to Nucl. Instrum. Methods Phys. Res., Sect. B.
  - [31] D. B. Cassidy and A. P. Mills, Nucl. Instrum. Methods Phys. Res., Sect. A **580**, 1338 (2007).
  - [32] K. P. Ziock, C. D. Dermer, R. H. Howell, F. Magnotta, and K. M. Jones, J. Phys. B: At., Mol. Opt. Phys. **23**, 329 (1990).
  - [33] S. Cialdi, I. Boscolo, F. Castelli, F. Villa, G. Ferrari, and M. Giammarchi, Nucl. Instrum. Methods Phys. Res., Sect. B **269**, 1527 (2011).
  - [34] F. Villa, Laser system for positronium excitation to Rydberg levels for Aegis experiment, PhD thesis, Milano (2011).
  - [35] S. Mariazzi, L. Di Noto, G. Nebbia and R. S. Brusa, J. of Phys.: Conf. Ser. **618**, 012039 (2015).
  - [36] Z. Mazzotta, R. Caravita, and F. Castelli, private communication.
  - [37] F. Castelli, Eur. Phys. J. Special Topics **203**, 137 (2012).